J. Biochem. **136**, 813–823 (2004)
DOI: 10.1093/jb/mvh191

DNA Condensation Monitoring after Interaction with Hoechst 33258 by Atomic Force Microscopy and Fluorescence Spectroscopy

Masato Saito, Masaaki Kobayashi, Shin-ichiro Iwabuchi, Yasutaka Morita, Yuzuru Takamura and Eiichi Tamiya*

School of Materials Science, Japan Advanced Institute of Science and Technology, 1-1 Asahidai, Tatsunokuchi, Ishikawa 923-1292

Received July 23, 2004; accepted October 1, 2004

DNA condensation was only observed after the addition of Hoechst 33258 (H33258) among various types of DNA binding molecules. The morphological structural change of DNA was found to depend on the H33258 concentration. On comparison of fluorescence spectrum measurements with AFM observation, it was found that fluorescence quenching of DNA-H33258 complexes occurred after DNA condensation. Additionally, we showed that DNA condensation by H33258 was independent of sequence selectivity or binding style using two types of polynucleotides, *i.e.* poly(dA-dT)·poly(dA-dT) and poly(dG-dC)·poly(dG-dC). Moreover, it was concluded that the condensation was caused by a strong hydrophobic interaction, because the dissolution of condensed DNA into its native form on dimethyl sulfoxide (DMSO) treatment was observed. This study is the first report, which defines the DNA condensation mechanism of H33258, showing the correlation between the single molecule scale morphology seen on AFM observation and the bulky scale morphology observed on fluorescence spectroscopy.

Key words: AFM, condensation, DNA, fluorescence, Hoechst 33258.

The bis-benzimidazole dye Hoechst 33258 (H33258): 2′-(4-hydroxyphenyl)-5-[5-(4-methylpiperazine-1-yl) benzimidazo-2-yl]-benzimidazole], is a well-described and widely used molecule in biochemical applications. H33258 has a flexible, long molecule with a positively charged end, and a number of proton donor and acceptor groups with possible hydrogen bonds between them. It was not only developed and used as an anticancer drug (*1–4*), but has also been applied as a fluorescent dye for nuclei staining (*5–7*). Furthermore, it is an electrochemically active compound (*8*). The electrochemical behavior of Hoechst 33258, *i.e.* its interaction with DNA, has been studied by means of several electrochemical techniques (*8*, *9*). There have been numerous reports on characterization of the DNA-H33258 interaction. NMR (*10*, *11*) and X-ray crystallography (*12*) studies showed that H33258 could bind in the minor grooves of AT-rich regions of DNA. The sequence-specific affinity of H32358 has been measured by massive parallel analysis with a generic microchip, and it was reported that AATT was the most favored binding site among various sequences (*13*). However, it has been suggested that H33258 has two different types of binding modes. Light scattering and fluorescence studies (*14*) showed that H33258 could bind to an AT-rich minor groove region specifically at a low DNA binding reagent/phosphate groups of DNA backbone (D/P) ratio, and then that fluorescence quenching occurred at a high D/P ratio. The non-specific binding of H33258 with DNA suggested by fluorescence and absorption studies (*15*) was supported by a titration rotational viscometric study (*16*). Although H33258's affinity to an AT region was reported to be higher than that to a GC region (*15*, *17*), it also exhibits weak affinity to a GC region. Furthermore, an electric linear dichroism study (*18*) demonstrated that H33258 exhibited unspecific binding ability as to GC-rich sequences as an intercalator.

DNA condensation plays an important role in DNA packing in a living cell or in the head of a bacteriophage (*19*). In addition, condensed DNA has been applied to gene therapy as a non-viral vector (*20*, *21*). DNA condensation can be induced by the addition of various condensing agents or combinations (*22*). In particular, characteristic condensed forms, i.e. a toroidal or rod-like shape, were observed when DNA was induced by multivalent cationic agents, for example, spermidine (*23*), poly-lysine (*24*), protamine (*25*), cobalt hexamine (*26*), and cationic silane (*27*, *28*). To investigate DNA condensation, various techniques, including vibrational CD (*29*), electron microscopy (*30*), light scattering (*31*), fluorescence microscopy (*32*), and pulse gel electrophoresis (*33*), have been used. Analysis involving simulation has also been performed (*34*). In addition to these techniques, atomic force microscopy (AFM) is a powerful tool for observing DNA condensation on the single molecule scale (*23–26*, *28*, *35*), because AFM can visualize DNA condensates in three dimensions with subnanometer height resolution and reflect near-physiological conditions in sample preparations. Thus, DNA condensation can easily be analyzed by AFM, and the results will deepen our understanding of this phenomenon.

We attempted to visualize the morphology of DNA with H33258 by AFM imaging. Many kinds of drugs, for example, methylene blue and propidium iodide as intercalators, and chromomycin A3, distamycin, 4′,6-diamidino-2-phenylindole dichloride (DAPI), berenil and H33258 as groove binders (*36*), were applied to DNA. As a result, we

*To whom correspondence should be addressed. E-mail: tamiya@jaist.ac.jp

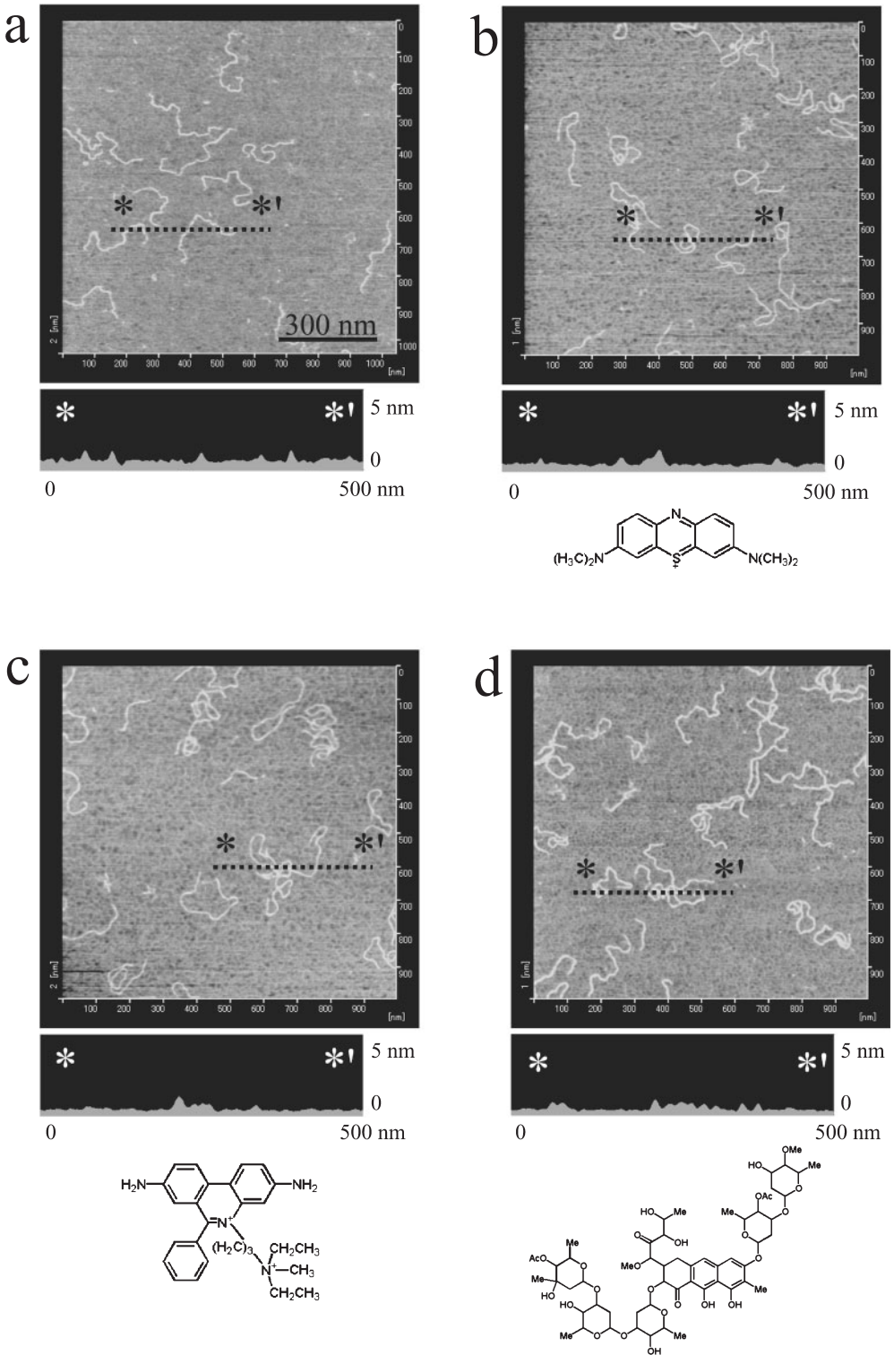

found that the DNA condensation was mostly highly induced by H33258 among all the above. To obtain a further understanding of the morphological change on DNA condensation with H32358, we investigated the effect of the H33258 concentration. Then, although H33258 is a mono-cationic molecule at pH 7.0 (*37–39*), we found that DNA took on characteristic forms induced by H33258 known as a toroidal or rod-like shape. Additionally, by comparing AFM images, fluorescence quenching was observed under the same sample conditions at the start of DNA condensation with H33258. In this study, a direct correlation between the molecular scale morphology observed on AFM imaging and the bulky scale information as fluorescence intensity signals is reported for the first time.

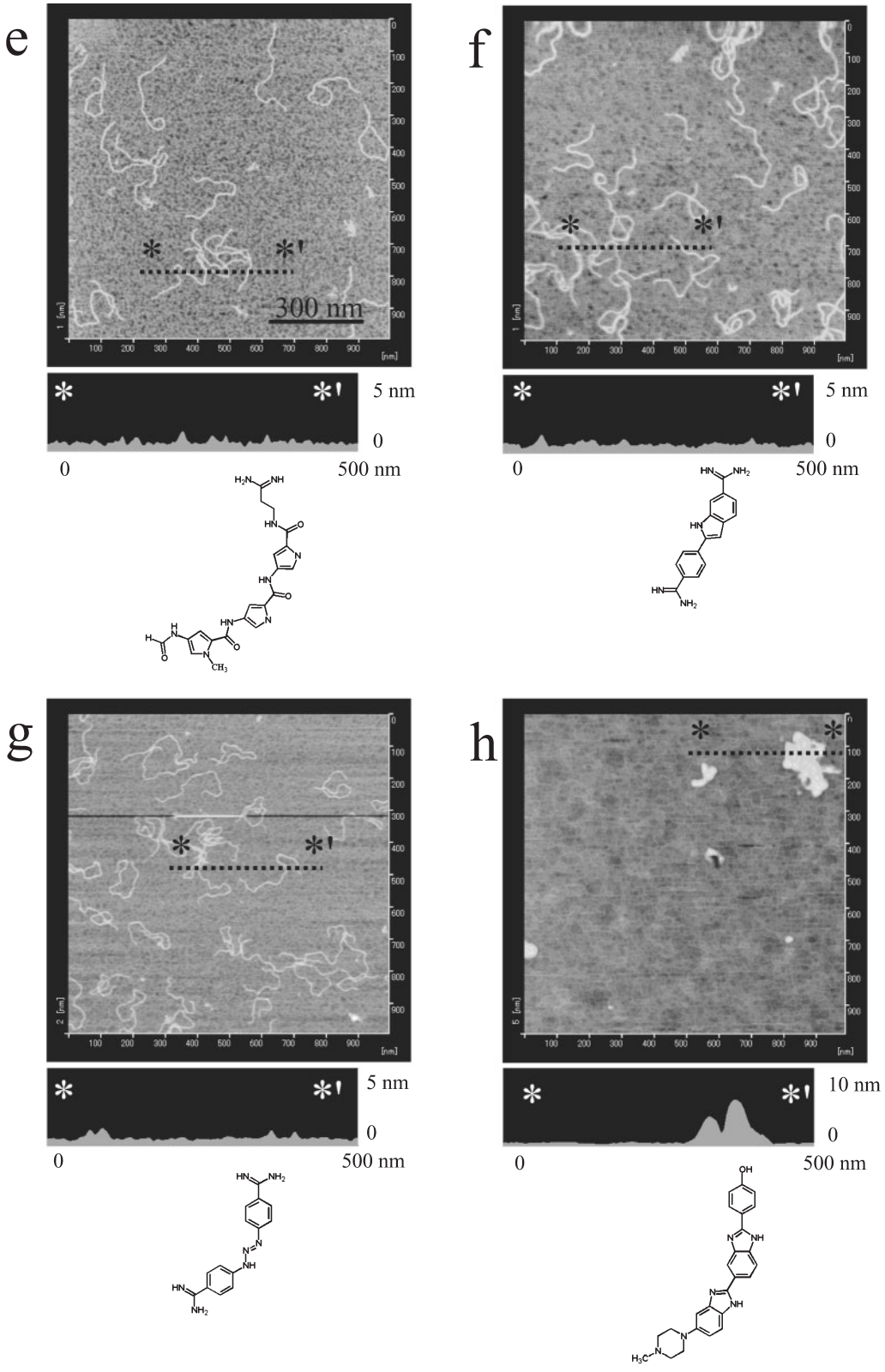

Fig. 1. **Chemical structures of intercalators and observation of DNA-intercalator complexes by AFM in air.** 1.5 nM 1000 bp DNA (3 μM phosphate of DNA) was mixed with various intercalators at 10 μM as follows: (a) no intercalator, (b) methylene blue, (c) propidium iodide (PI), (d) chromomycin A3, (e) distamycin, (f) 4′,6-diamidino-2-phenylindole dichloride (DAPI), (g) berenil, (h) Hoechst 33258 (H33258). All samples were prepared in a 10 mM phosphate buffer solution (pH 7.0) containing 100 mM NaCl and 1 mM EDTA. The scan size was 1,000 nm × 1,000 nm. The line profiles of all the DNA-small molecule complexes are shown under the corresponding AFM images.

Table 1. **DNA base sequences of primers and the PCR amplified product (1,000 bp).**

Forward primer: 5′-CAACTGATCTTCAGCATC-3′
Reverse primer: 5′-CACGACACTCATACTAAC-3′
1,000 bp DNA: 5′-CAACTGATCTTCAGCATCTTTTACTTTCACCAGCGTTTCTGGGTGAGCAAAAACAGGAAGGCAAAATGCCGCAAAAA AGGGAATAAGGGCGACACGGAAATGTTGAATACTCATACTCTTCCTTTTTCAATATTATTGAAGCATTTATCAGGGTTATTGTCTCATGA GCGGATACATATTTGAATGTATTTAGAAAAATAAACAAATAGGGGTTCCGCGCACATTTCCCCGAAAAGTGCCACCTGACGCGCCCTGT AGCGGCGCATTAAGCGCGGCGGGTGTGGTGGTTACGCGCAGCGTGACCGCTACACTTGCCAGCGCCCTAGCGCCCGCTCCTTTCGCT TTCTTCCCTTCCTTTCTCGCCACGTTCGCCGGCTTTCCCCGTCAAGCTCTAAATCGGGGGCTCCCTTTAGGGTTCCGATTTAGTGCTTT ACGGCACCTCGACCCCAAAAAACTTGATTAGGGTGATGGTTCACGTAGTGGGCCATCGCCCTGATAGACGGTTTTTCGCCCTTTGACG TTGGAGTCCACGTTCTTTAATAGTGGACTCTTGTTCCAAACTGGAACAACACTCAACCCTATCTCGGTCTATTCTTTTGATTTATAAGGG ATTTTGCCGATTTCGGCCTATTGGTTAAAAAATGAGCTGATTTAACAAAAATTTAACGCGAATTTTAACAAAATATTAACGCTTACAATT TCCATTCGCCATTCAGGCTGCGCAACTGTTGGGAAGGGCGATCGGTGCGGGCCTCTTCGCTATTACGCCAGCTGGCGAAAGGGGGAT GTGCTGCAAGGCGATTAAGTTGGGTAACGCCAGGGTTTTCCCAGTCACGACGTTGTAAAACGACGGCCAGTGACGGGCCCCCCCTCGA GTAATACGACTCACTATAGCCAGCCCCCGATTGGGGGCGACACTCCACCATAGATCACTCCCCTGTGAGGAACTACTGTCTTCACGCA GAAAGCGTCTAGCCATGGCGTTAGTATGAGTGTCGTG-3′

MATERIALS AND METHODS

Materials—H33258, methylene blue, propidium iodide (PI), chromomycin A3, distamycin, 4′,6-diamidino-2-phenylindole dichloride (DAPI), and berenil were purchased from Sigma Co. (St. Louis, MO, USA). Poly(dG-dC)·poly(dG-dC), with a molecular mass of 4.7×10^5, and poly(dA-dT)·poly(dA-dT), with a molecular mass of 1.98×10^6, were obtained from Amersham Biosciences Co. (Piscataway, NJ, USA). A DNA fragment of 1,000 bp length was obtained by PCR amplification from the segment of the Hepatitis C virus (HCV) DNA sequence cloned in plasmid pBluescriptII (from 12200 to 761 in 12,439 bp, 49.2 GC %). PCR was performed in a final volume of 50 μl using KOD DNA polymerase (Toyobo Co., Ltd., Osaka, Japan) under the standard conditions for KOD. The primers (Griner Japan, Japan) and amplified 1,000 bp DNA sequences are shown in Table 1. The HCV DNA sequences cloned in plasmid pBluescriptII were kindly provided by Prof. Syu-ichi Kaneko of the University of Kanazawa, Kanazawa City, Japan. After PCR amplification, DNA was purified by phenol/chroloform extraction and precipitation with ethanol, and then suspended in 10 mM Tris buffer (pH 8.0) containing 1mM EDTA. The DNA concentration was determined by absorbance measurement at 260 nm. DNA-reagent complexes were prepared by adding DNA to a reagent solution containing 10 mM phosphate buffer solution (pH 7.0, PBS), 100 mM NaCl and 1 mM EDTA. All DNA samples were diluted until a final concentration of 1.5 nM (*i.e.* 3 μM in terms of phosphate of nucleotides) was reached. The DNA binding reagents were also diluted to a final concentration between 0 and 10 μM. Thus, the D/P ratio was equal to 0–3.33. This mixture was incubated in the dark for 10 min at room temperature. All solutions were prepared and diluted with ultra pure (Milli Q) water.

AFM Imaging—Mica was purchased from Furuuchi Chemical Co. (Shinagawa, Tokyo, Japan). 3-aminopropyltriethoxysilane (APTES) was purchased from Chisso Co. (Chuo, Tokyo, Japan). To immobilize samples, a mica surface modified with APTES (AP-mica) was used as a substrate (*40*). DNA adheres to the imaging surface through electrostatic attraction. In the glove box with controlled ambient humidity, AP-mica was prepared by placing freshly cleaved mica into a 2 liter desiccator that contained 10 μl APTES for 2 h. The AP-mica was removed and baked at 120°C for 15 min. Then, the AP-mica was stored under vacuum prior to making samples. DNA-reagent solutions were deposited onto AP-mica. After 2 min, each mica disk was rinsed two times with 100 μl of ultra pure water, and then dried up under nitrogen gas weakly. All AFM images were obtained in air with a commercial AFM unit (SPA400-SPI3800. Seiko Instruments Inc., Chiba, Japan) equipped with a calibrated 20 μm *xy*-scan and 10 μm *z*-scan range PZT-scanner. A silicon nitride tip (SI-DF40, spring constant = 42 N/m. Seiko Instruments Inc.) was used, and images were taken in the dynamic force mode (DFM mode) at optimal force. All AFM operations were performed in the moisture control box at room temperature and 30–40% humidity.

Fluorescence Measurement—The fluorescence intensity of the DNA-H33258 complex was measured with a Spectrofluorometer FP-777 (JASCO, Tokyo, Japan). Excitation was performed at 360 nm of the Xe line, and fluorescent profiles were recorded by scanning the emission from 400 to 600nm. The fluorescence intensity data were collected from emission spectra obtained at 460 and 510 nm.

RESULTS AND DISCUSSION

Observation of DNA-DNA Binding Reagent Complexes by AFM—The morphological changes of complexes caused by the addition of various types of DNA binding reagents to DNA were examined by AFM imaging. In the absence of a DNA binding reagent, the typical native form of 1,000 bp DNA molecules is shown in Fig. 1A. Assuming that DNA was in the B form, the theoretical length of 1,000 bp was taken as 340 nm, and almost all the DNA lengths in Fig. 1A are in agreement with this assumption. The AFM images in Fig. 1B show DNA bound with methylene blue, which exhibits affinity to a GC-rich region (*41*), and those in Fig. 1C show DNA bound with propidium iodide, which is known as a site-nonspecific intercalator (*42*). Figure 1D shows chromomycin A3 as a minor groove binder of a GC-rich region (*43*). Figure 1E shows distamycin, which exhibits affinity to the grooves of both AT-rich and GC-rich regions (*44*). DAPI (*45*) and berenil (*46*, *47*), as AT-rich groove binders, are shown in Fig. 1, F and G, respectively. A significant morphological change in DNA was not observed when these reagents were applied. However, when H33258, as an AT-rich binder, was used, DNA clearly condensed (Fig. 1H). Although H33258 and other reagents are known to interact with DNA as DNA binders, this condensation of DNA only occurred on the addition of H33258 to it. Addition-

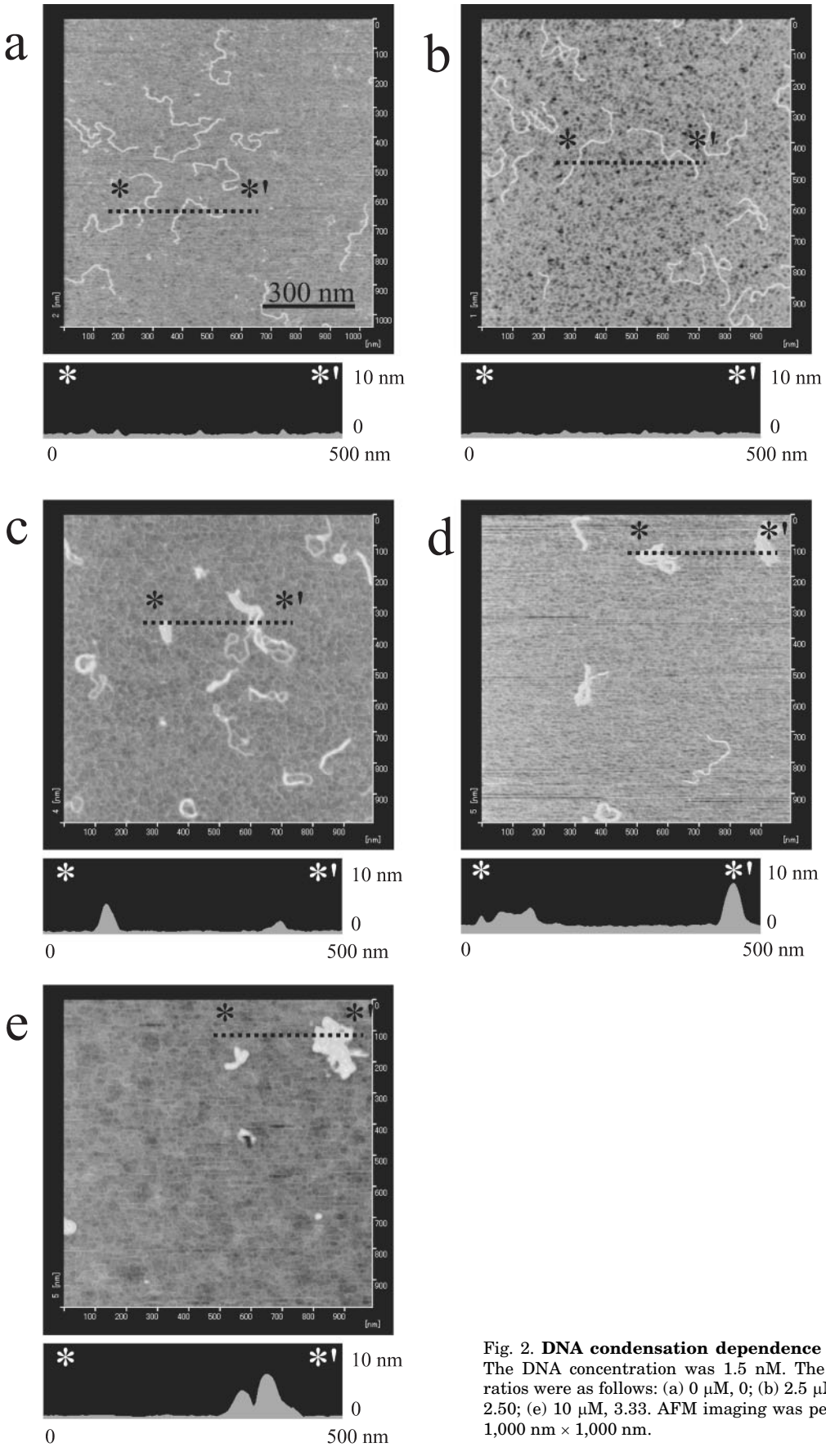

Fig. 2. **DNA condensation dependence on the H33258 concentration.** The DNA concentration was 1.5 nM. The H33258 concentrations and D/P ratios were as follows: (a) 0 μM, 0; (b) 2.5 μM, 0.83; (c) 5 μM, 1.67; (d) 7.5 μM, 2.50; (e) 10 μM, 3.33. AFM imaging was performed in air with a scan size of 1,000 nm × 1,000 nm.

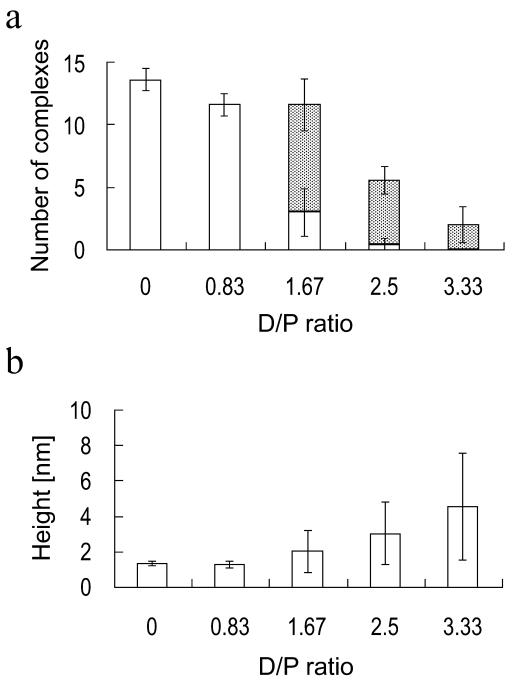

Fig. 3. **The number and height of condensed DNA complexes dependent on the H33258 concentration.** Histograms show the number (a) and height (b) of the complexes adsorbed onto the substrate. The number of samples per 1,000 nm × 1,000 nm was determined from five consequtive AFM images, as shown in Fig. 2, under the same D/P ratio conditions. The height was determined from the maximum vertical interval, which clipped 10–12 samples from AFM images randomly.

ally, the line profile of the DNA condensate with H33258 revealed that the height increased to 5.52 nm (inset in Fig. 1h) relative to DNA, and with the other reagents to 0.61 and 0.88 nm (insets in Fig. 1, a–g). Thus, it was thought that the DNA-H33258 complex contained several DNA molecules in comparison with other DNA forms.

The Morphological Changes of DNA Depend on the H33258 Concentration and Characteristic Condensed Structures—The morphological change on DNA condensation, that accompanied the H33258 concentration-dependence, was investigated by AFM imaging. The DNA form after adding 2.5 μM H33258 (Fig. 2b, D/P ratio: 0.83) was similar to the native one (Fig. 2a). With 5.0 μM H33258 (D/P ratio: 1.67), various DNA forms, for example a condensate and also ones similar to the native form, were observed (Fig. 2c). The DNA condensate obtained with 7.5 μM H33258 (Fig. 2d, D/P ratio: 2.50) was larger than that with 5.0 μM in Fig. 2c. Complete condensation of DNA was observed on the addition of 10.0 μM H33258 (Fig. 2e, D/P ratio: 3.33). The morphological change of condensed DNA was found to exhibit H33258 concentration-dependence.

Figure 3a shows to the extent of native or condensed DNA adsorption onto the substrate shown in Fig. 2. A histogram shows the averages for an adsorbed sample, which was determined from 5 AFM images for each D/P ratio. Figure 3b shows the height for native or condensed DNA, 10–12 samples being scanned randomly. The heights were determined from the maximum vertical interval in clipped sample images. The number for adsorbed DNA without H33258 at the D/P ratio of 0 was 13.60 ± 0.89 (mean ± SD) samples per 1,000 nm × 1,000 nm. The height was 1.36 ± 0.12 nm. The number for DNA in the presence of 2.5 μM H33258 at the D/P ratio of 0.83 was found to be 11.60 ± 0.86 samples, and the height was 1.29 ± 0.20 nm. At the D/P ratio of 1.67, the total number of adsorbed samples was 11.60 ± 1.67. In particular, 8.6 ± 2.07 (74.14%) samples, which gave small condensed forms, appeared at this concentration. The height slightly increased to 2.03 ± 1.17 nm along with the condensation of DNA. With the D/P ratio of 2.50, the number of adsorbed samples decreased remarkably to 5.60 ± 1.14, which gave larger condensed forms, which included 5.20 ± 1.09 (92.86%) resulting from the increase of 3.04 ± 1.74 nm in height. With the D/P ratio of 3.33, DNA condensation became greater (4.57 ± 3.00 nm) and adsorption decreased to 2.0 ± 1.41 samples (100% condensed forms). Many samples could adsorb on the surface with low H33258 concentrations, and the condensed shapes were small on the exterior. However, as the H33258 concentration increased, the condensed shapes became larger, but the number of adsorbed DNA samples decreased. In other words, it was thought that H33258 could cause inter-molecular condensation at 10 μM, whereas it could only cause intra-molecular condensation of single DNA at 5 μM.

Various types of characteristic condensates related to DNA-H33258 complexes are shown in Fig. 2c, and thus AFM imaging of the same sample was performed. We found that DNA could change to its characteristic shapes, *i.e.* toroid, rod, globule, and worm (Fig. 4). Generally, these shapes have been well-described as DNA condensation by tri- or tetravalence cationic molecules (*22–26*). In our study, it was found that DNA could form a toroidal or rod-like shape after interaction with H33258, although it was a monovalent cation in neutral solution (*37–39*).

Fluorescence Detection of DNA-H33258 Complexes under the Same Conditions as for AFM Imaging—In order to observe DNA condensation with H33258, the fluorescence of bound and free H33258 was measured under the same conditions in bulk solutions that were used for AFM imaging. The results were compared to the respective AFM images for each D/P ratio. At neutral pH, free H33258 that was excited in 360 nm exhibited weak fluorescence around 510 nm, but upon binding to DNA, the fluorescence efficiency increased and the emission shifted to 460 nm (*5*). Figure 5 shows the fluorescence intensity plotted versus the increase in H33258 concentration as the D/P ratio for free H33258 at 510 nm (open circles), and DNA-H33258 complexes at 460 nm (black squares) and also at 510 nm (black circles). The fluorescence intensity of free H33258 at 510 nm increased linearly with the increase in H33258 concentration. The fluorescence intensity of the DNA-H33258 complexes at 460 nm reached a maximum at the D/P ratio of 0.83. In comparison with the respective AFM image in Fig. 2b, DNA molecules were still close to their native form. However, the fluorescence intensity of the DNA-H33258 complex began to decrease and quenched as the D/P ratio increased. Then, an interesting phenomenon, *i.e.* the fluorescence of free H33258 became higher than that of the bound species at 510 nm, was observed at the D/P ratio of

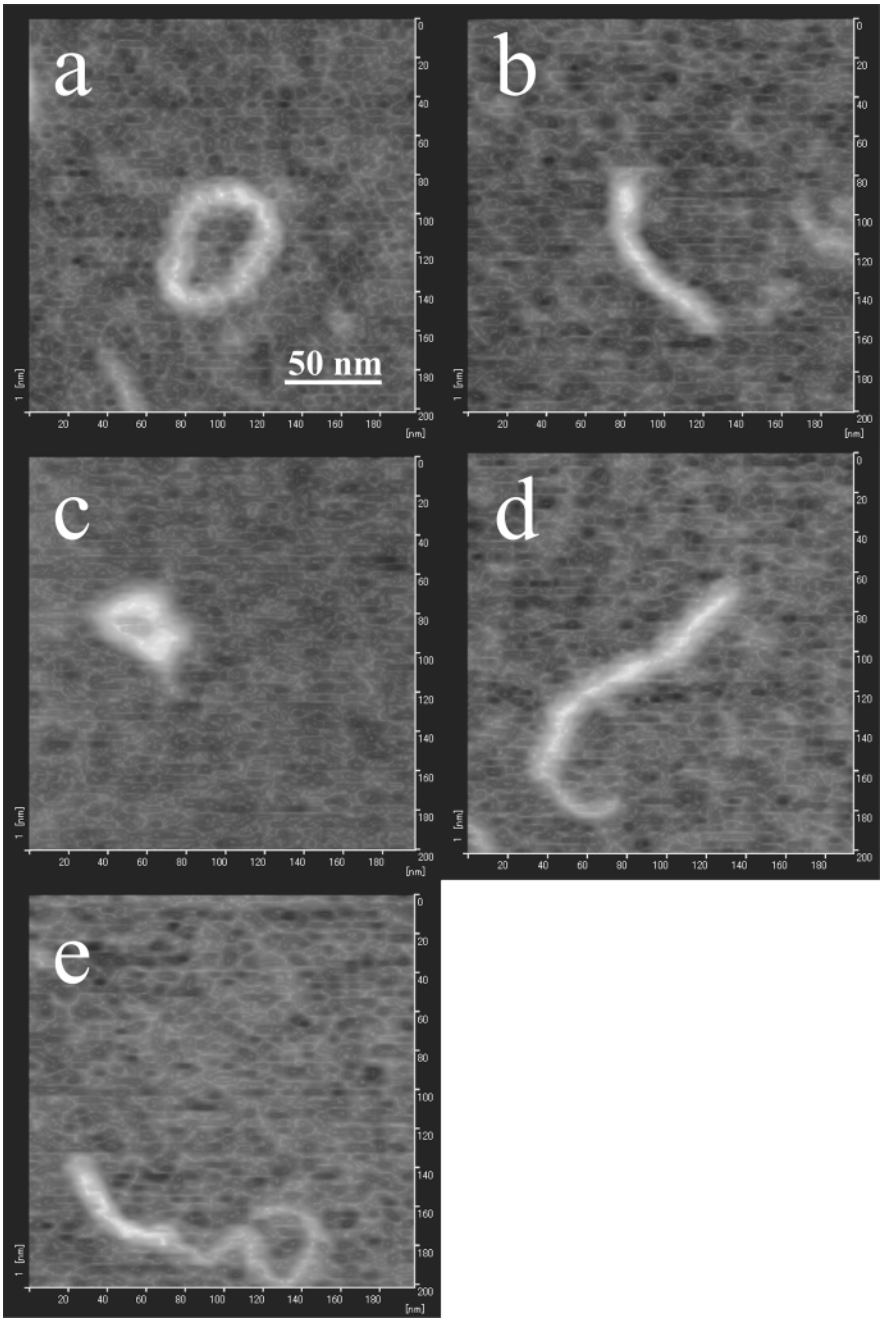

Fig. 4. **Characteristic shapes of DNA-H33258 complexes.** Several condensed structures, for example, toroidal (a), rod-like (b), globule (c), and worm-like (d, e), were observed under the condensation conditions in Fig. 2c with the scan size of 200 nm × 200 nm.

1.67. In this condition, we found that DNA formed condensed forms with H32358 on AFM imaging, as shown in Fig. 2c. After the D/P ratio of 1.67, DNA condensation occurred (Fig. 2, d and e), and thus the fluorescence intensity was still lower than that of free H33258. As expected, the fluorescence measurements involving 10 mM Tris buffer solution (pH 7.0) showed a similar dependence (data not shown).

Figure 6 shows the fluorescence measurements for free dyes: DAPI at 457 nm (squares), propidium iodide (PI) at 615 nm (triangles), and H33258 at 510 nm (circles), in the range of 0 to 1,500 μM at neutral pH. The fluorescence intensity of DAPI and PI increased with increasing concentrations, saturation being reached at 500 μM and 1000 μM, respectively. Although the fluorescence of H33258 reached a maximum at around 100 μM, with higher concentrations, its fluorescence decreased, becoming below half the maximum. This result showed that only H33258 had the property of concentration quenching amongst the other dyes.

Condensation of Polynucleotides in the Presence of H33258—In order to investigate the sequence specificity of DNA condensation by H33258, synthetic polynucleotides with alternating structures: poly(dA-dT)·poly(dA-dT) and poly(dG-dC)·poly(dG-dC), were used. Complexes were prepared by adding polynucleotides to a H33258 solution in 10 mM PBS with 100 mM NaCl. The final concentrations of H33258 and polynucleotides were 10 μM and 3 μM in terms of phosphate groups of nucleotides for both the polynucleotides, respectively. It was found that

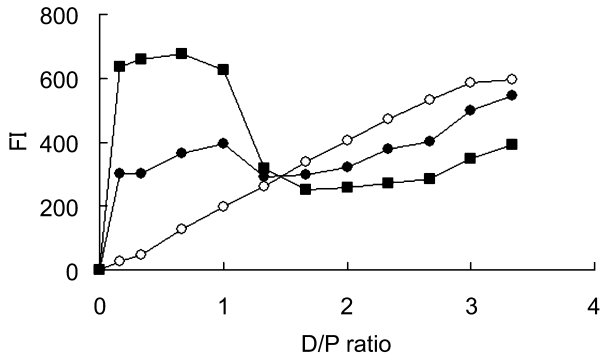

Fig. 5. **Fluorescence measurement of DNA-H33258 complex dependence on the H33258 concentration.** All samples contained 1.5 nM 1000 bp DNA (in terms of 3 μM phosphate) in PBS under the same conditions as for AFM measurement in Fig. 1. The fluorescence of H33258 with DNA at 460 nm (black squares) and 510 nm (black circles), and only H33258 without DNA at 510 nm (open circles) was plotted. Excitation was performed at 360 nm. The photomultiplier gain was set at medium. D/P ratio is the ratio between the mole of DNA binding reagent (H33258) and the mole of DNA phosphate.

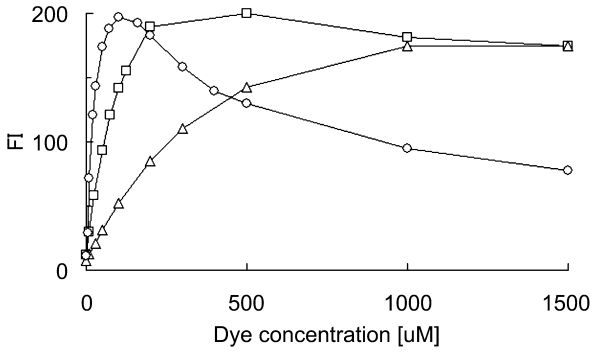

Fig. 6. **Self-fluorescence intensity dependence upon the dye concentration.** The fluorescence intensity in peak wavelength was plotted graphically as follows; 4′,6-diamidino-2-phenylindole dichloride (DAPI) at 457 nm (squares), propidium iodide (PI) at 615 nm (triangles), and H33258 at 510 nm (circles). The photomultiplier gain was set at low.

H33258 could condense both polynucleotides into higher ordered structures (Fig. 7). Poly(dA-dT)·poly(dA-dT) in the presence of H33258 produced globules (Fig. 7a), and poly(dG-dC)·poly(dG-dC) in the presence of H33258 produced toroids, worms, and globules (Fig. 7c). Additionally, in both cases, large condensates, considered to be caused by intermolecular condensation, were also observed.

The Process of DNA Condensation with H33258—As shown in Fig. 2, it was observed that DNA condensation depended on the H33258 concentration, and the size of the condensate also became grater in proportion to the concentration. Additionally, on comparing these AFM images with the results of fluorescence measurements in Fig. 5, it was found that fluorescence quenching occurred after DNA condensation. Here, it should be noted that the fluorescence intensity with the H33258 concentration that yielded a condensate at a D/P ratio of 1.67 or more became lower than that of free H33258 at the same concentration at both 460 nm and 510 nm. On the other hand, free H33258 had the nature that yielded the concentration quenching at higher concentrations of 100 μM as shown in Fig. 6. This phenomenon also occurred when a Tris buffer solution was used (data not shown). These results show that the amount of H33258 used for the condensation, which showed a decrease in fluorescence intensity, existed in the surroundings of DNA locally and excessively. Thus, this phenomenon could be considered as concentration quenching of the condensate.

In this study, various types of DNA binding molecules were allowed to interact with DNA, and we observed their morphological structures by AFM. DNA condensation was only observed after the addition of H33258. In general, DNA condensation is known to occur with multivalent cationic molecules (*22–28*). Utsuno *et al.* (*48*) also showed the possibility of aggregation of DNA via H33258 by AFM imaging, and discussed the trivalent cation of H33258. However, it has been reported that H33258 has the nature of a monovalent cation under neutral conditions (*37–39*). Here, H33258 was also considered to be a monovalent cation, and that this property was the factor that caused DNA condensation.

As shown in Fig. 1, the condensation did not occur after the intercalation of methylene blue or propidium iodide, or groove binding with chromomycin A3, distamycin, DAPI, or berenil. It was concluded that the binding mode of reagents did not contribute to DNA condensation. Additionally, the condensation also did not occur with the bivalent cations propidium iodide, DAPI, and berenil, which all exhibited more valency than the monovalent H33258. It was concluded that there was no direct participation of the valency of the binding molecule to the condensation.

On the other hand, it has been well described that H33258 bound strongly to the minor groove of an AT region, and weakly to a GC region as an intercalator (*15*, *17*, *18*). It was thought that the sequence recognition or binding style of H33258 as to DNA would affect DNA condensation. Both types of polynucleotides, *i.e.* poly(dA-dT)·poly(dA-dT) and poly(dG-dC)·poly(dG-dC), formed condensates with H33258, as shown in Fig. 7. The H33258 concentration at which the condensation started for both polynucleotides was found to be 2.5 μM. We employed 10 μM H33258 for condensation of a PCR-amplified DNA sample in this study, so it was confirmed that H33258 at such a high concentration did not show any sequence-specificity. Our results showed that DNA condensation by H33258 could be monitored independent of sequence recognition, ligand concentration or binding style.

How can a DNA condensate be produced by H33258? An unknown property of H33258 might be the reason for DNA condensation. H33258 consists of a phenol, a piperazine, and two benzimide rings, and therefore it is strongly hydrophobic. Its hydrophobic nature might be the cause of DNA condensation. In fact, a hydrophobic environment is created by excessive H33258 localized around DNA, thus condensation occurs through a strong hydrophobic interaction. The mode of this condensation may be close to the condensation mechanism of cationic lipids, which was reported by Matulis *et al.* (*49*), and Reimer *et al.* (*50*). In order to support our hypothesis of condensation through hydrophobic interaction, we tried

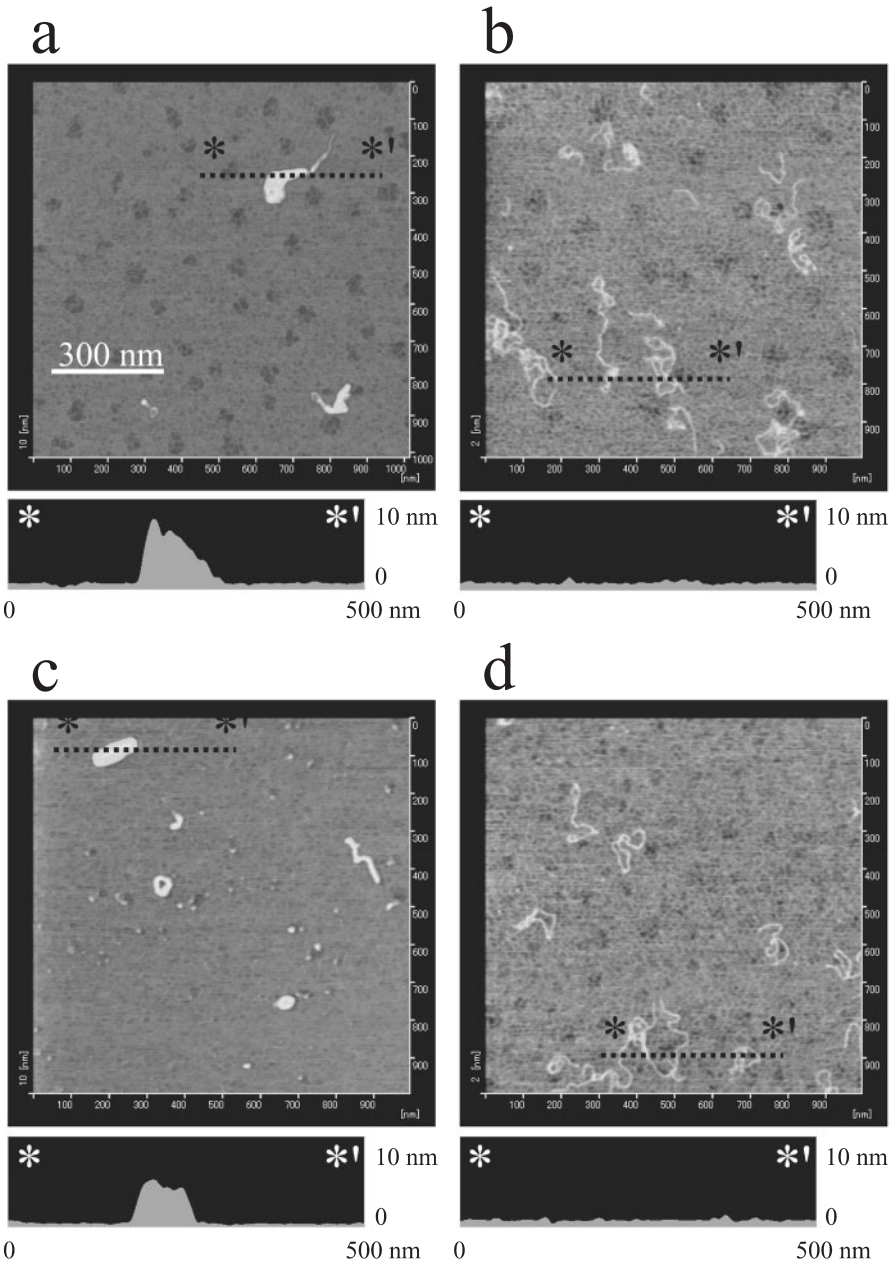

Fig. 7. **AFM images for structural comparison of the native and condensed forms of polynucleotides in the presence and absence of H33258.** AFM images show poly(dA-dT)·poly(dA-dT) with (a) and without (b) H33258, and poly(dG-dC)·poly(dG-dC) with (c) and without (d) H33258. 1 ng/μl DNA (3 μM phosphate of DNA) was mixed with a 10 μM H33258 solution containing 10 mM PBS (pH 7.0), 100 mM NaCl, and 1 mM EDTA, with a scan size of 1000 nm × 1,000 nm.

the addition of 5% DMSO as an organic solvent to the condensed DNA, and imaged by AFM. As a result, the condensate was completely dissolved, and DNA returned to its native form (data not shown). Stokke and Steen (*14*) reported that the addition of 25% ethanol to DNA in the presence of a high H33258 concentration, which caused fluorescence quenching, restored the fluorescence and reduced the amount of light scattering. Hence, it was thought that condensation *via* H33258 involved many factors for hydrophobic interactions.

The process of DNA condensation with H32358 can be concluded to be as follows. H33258 approaches DNA due to monovalency, and binds to the minor groove of AT-rich region at low H33258 concentrations. After the AT regions have been filled, more H33258 interacts with the GC-rich regions as an intercalator. Then, excessive H33258 remains confined randomly around DNA due to its monovalency. Thus, concentration quenching is observed. Finally, the hydrophobic environment created by excessive H33258 might induce DNA condensation.

CONCLUSION

H33258 is an attractive molecule that has an anti-cancer effect as well as unique fluorescence and electrochemical activities. The interaction of H33258 with DNA, which showed multi-binding modes and fluorescence quenching, has been discussed in detail. In this paper, two important findings are presented for DNA condensation with H33258. First is the finding that a DNA condensate could form without sequence specificity by using both polynucleotides, *i.e.* poly(dA-dT)·poly(dA-dT) and poly(dG-dC)·poly(dG-dC). The second finding is the correlation between the observation of DNA condensation with

H33258 using AFM on the single molecule scale and the measurement of fluorescence characteristics quantitatively. Condensation caused by H33258 is further discussed, and a possible mechanism is proposed.

REFERENCES

1. Reddy, B.S., Sharma, S.K., and Lown, J.W. (2001) Recent developments in sequence selective minor groove DNA effectors. *Curr. Med. Chem.* **8**, 475–508
2. Tolner, B., Hartley, J.A., and Hochhauser, D. (2001) Transcriptional regulation of topoisomerase II alpha at confluence and pharmacological modulation of expression by bis-benzimidazole drugs. *Mol. Pharmacol.* **59**, 699–706
3. Denny, W.A. (2001) DNA minor groove alkylating agents. *Curr. Med. Chem.* **8**, 533–544
4. Bailly, C. (2000) Topoisomerase I poisons and suppressors as anticancer drugs. *Curr. Med. Chem.* **7**, 39–58
5. Latt, S.A. and Wohlleb, J.C. (1975) Optical studies of the interaction of 33258 Hoechst with DNA, chromatin, and metaphase chromosomes. *Chromosoma* **52**, 297–316
6. Hilwig, I. and Gropp, A. (1975) pH-dpendent fluorescence of DNA and RNA in cytologic staining with "33258" Hoeschst. *Exp. Cell Res.* **91**, 457–460
7. Yamamoto, A., Araki, T., Fujimori, K., Yamada, M., Yamaguchi, H., Izumi, K., and Matsumoto, K. (1989) NaCl-aided Hoechst 33258 staining method for DNA quantification and its application. *Histochemistry* **92**, 65–68
8. Hashimoto, K., Ito, K., and Ishimori, Y. (1994) Sequence-specific gene detection with a gold electrode modified with DNA probes and an electrochemically active dye. *Anal. Chem.* **66**, 3830–3833
9. Hashimoto, K. and Ishimori, Y. (2001) Preliminary evaluation of electrochemical PNA array for detection of single base mismatch mutations. *Lab on a Chip* **1**, 61–63
10. Gavathiotis, E., Sharman, G.J., and Searle, M.S. (2000) Sequence-dependent variation in DNA minor groove width dictates orientational preference of Hoechst 33258 in A-tract recognition: solution NMR structure of the 2:1 complex with d(CTTTTGCAAAAG)(2). *Nucleic Acids Res.* **28**, 728–735
11. Harris, S.A., Gavathiotis, E., Searle, M.S., Orozco, M., and Laughton, C.A. (2001) Cooperativity in drug-DNA recognition: a molecular dynamics study. *J. Amer. Chem. Soc.* **123**, 12658–12663
12. Squire, C.J., Baker, L.J., Clark, G.R., Martin, R.F., and White, J. (2000) Structures of m-iodo Hoechst-DNA complexes in crystals with reduced solvent content: implications for minor groove binder drug design. *Nucleic Acids Res.* **28**, 1252–1258
13. Drobyshev, A.L., Zasedatelev, A.S., Yershov, G.M., and Mirzabekov, A.D. (1999) Massive parallel analysis of DNA-Hoechst 33258 binding specificity with a generic oligodeoxyribonucleotide microchip. *Nucleic Acids Res.* **27**, 4100–4105
14. Stokke, T. and Steen, H.B. (1985) Multiple binding modes for Hoechst 33258 to DNA.*J. Histochem. Cytochem.* **33**, 333–338
15. Loontiens, F.G., Regenfuss, P., Zechel, A., Dumortier, L., and Clegg, R.M. (1990) Binding characteristics of Hoechst 33258 with calf thymus DNA, poly[d(A-T)], and d(CCGGAATTCCGG): multiple stoichiometries and determination of tight binding with a wide spectrum of site affinities. *Biochemistry* **29**, 9029–9039
16. Steinmetzer, K. and Reinert, K.E. (1998) Multimode interaction of Hoechst 33258 with eukaryotic DNA; quantitative analysis of the DNA conformational changes. *J. Biomol. Struct. Dyn.* **15**, 779–791
17. Bailly, C., Colson, P., Henichart, J.P., and Houssier, C. (1993) The different binding modes of Hoechst 33258 to DNA studied by electric linear dichroism. *Nucleic Acids Res.* **21**, 3705–3709
18. Colson, P., Houssier, C., and Bailly, C. (1995) Use of electric linear dichroism and competition experiments with intercalating drugs to investigate the mode of binding of Hoechst 33258, berenil and DAPI to GC sequences. *J. Biomol. Struct. Dyn.* **13**, 351–366
19. Wolffe, A. (1995) *Chromatin: Structure and Function*, Academic Press, London
20. Kay, M.A., Liu, D., and Hoogerbrugge, P.M. (1997) Gene therapy. *Proc. Natl Acad. Sci. USA* **94**, 12744–12746
21. Davis, M.E. (2002) Non-viral gene delivery systems. *Curr. Opin. Biotechnol.* **13**, 128–131
22. Bloomfield, V.A. (1996) DNA condensation. *Curr. Opin. Struct. Biol.* **6**, 334–341
23. Lin, Z., Wang, C., Feng, X., Liu, M., Li, J., and Bai, C. (1998) The observation of the local ordering characteristics of spermidine-condensed DNA: atomic force microscopy and polarizing microscopy studies. *Nucleic Acids Res.* **26**, 3228–3234
24. Golan, R., Pietrasanta, L.I., Hsieh, W., and Hansma, H.G. (1999) DNA toroids: stages in condensation. *Biochemistry* **38**, 14069–14076
25. Balhorn, R., Brewer, L., and Corzett, M. (2000) DNA condensation by protamine and arginine-rich peptides: analysis of toroid stability using single DNA molecules. *Mol. Reprod. Dev.* **56**, 230–234
26. Liu, D., Wang, C., Li, J., Lin, Z., Tan, Z., and Bai, C. (2000) Atomic force microscopy analysis of intermediates in cobalt hexammine-induced DNA condensation. *J. Biomol. Struct. Dyn.* **18**, 1–9
27. Fang, Y. and Hoh, J.H. (1998) Surface-directed DNA condensation in the absence of soluble multivalent cations. *Nucleic Acids Res.* **26**, 588–593
28. Fang, Y. and Hoh, J.H. (1999) Cationic silanes stabilize intermediates in DNA condensation. *FEBS Lett.* **459**, 173–176
29. Andrushchenko, V., Leonenko, Z., Cramb, D., van de Sande, H., and Wieser, H. (2001) Vibrational CD (VCD) and atomic force microscopy (AFM) study of DNA interaction with Cr^{3+} ions: VCD and AFM evidence of DNA condensation. *Biopolymers* **61**, 243–260
30. Arscott, P.G., Ma, C., Wenner, J.R., and Bloomfield, V.A. (1995) DNA condensation by cobalt hexaammine(III) in alcohol-water mixtures: dielectric constant and other solvent effects. *Biopolymers* **36**, 345–364
31. He, S., Arscott, P.G., and Bloomfield, V.A. (2000) Condensation of DNA by multivalent cations: experimental studies of condensation kinetics. *Biopolymers* **53**, 329–341
32. Takahashi, M., Yoshikawa, K., Vasilevskaya, V.V., and Khokhlov, A.R. (1997) Discrete coil-globule transition of single duplex DNAs induced by polyamines. *J. Phys. Chem. B* **101**, 9396
33. Li, A.Z., Qi, L.J., Shih, H.H., and Marx, K.A. (1996) Trivalent counterion condensation on DNA measured by pulse gel electrophoresis. *Biopolymers* **38**, 367–376
34. Stevens, M.J. (2001) Simple simulations of DNA condensation. *Biophys. J.* **80**, 130–139
35. Hansma, H.G. (2001) Surface biology of DNA by atomic force microscopy. *Annu. Rev. Phys. Chem.* **52**, 71–92
36. Geierstanger, B.H. and Wemmer, D.E. (1995) Complexes of the minor groove of DNA. *Annu. Rev. Biophys Biomol. Struct.* **24**, 463–493
37. Aleman, C., Adhikary, A., Zanuy, D., and Casanovas, J. (2002) On the protonation equilibrium for the benzimidazole derivative Hoechst 33258: an electronic molecular orbital study. *J. Biomol. Struct. Dyn.* **20**, 301–310
38. Gorner, H. (2001) Direct and sensitized photoprocesses of bisbenzimidazole dyes and the effects of surfactants and DNA. *Photochem. Photobiol.* **73**, 339–348
39. Kalninsh, K.K., Pestov, D.V., and Roshchina, Y.K. (1994) Absorption and fluorescence spectra of the probe Hoechst 33258. *J. Photochem. Photobiol. A* **83**, 39–47
40. Bezanilla, M., Manne, S., Laney, D.E., Lyubchenko, Y.L., and Hansma, H.G. (1995) Adsorption of DNA to mica, silylated mica, and minerals: Characterization by atomic force microscopy. *Langmuir* **11**, 655–659

41. Rohs, R., Sklenar, H., Lavery, R., and Roder, B. (2000) Methylene blue binding to DNA with alternating GC base sequence: A modeling study. *J. Amer. Chem. Soc.* **122**, 2860–2866
42. Casu, M., Puligheddu, S., Saba, G., Marincola, F.C., Orellana, G., and Lai, A. (1997) The interaction of DNA with intercalating agents probed by sodium-23 NMR relaxation rates. *J. Biomol. Struct. Dyn.* **15**, 37–43
43. Chakrabarti, S., Mir, M.A., and Dasgupta, D. (2001) Differential interactions of antitumor antibiotics chromomycin A(3) and mithramycin with d(TATGCATA)(2) in presence of Mg(2+). *Biopolymers* **62**, 131–140
44. Wemmer, D.E. (2000) Designed sequence-specific minor groove ligands. *Annu. Rev. Biophys Biomol. Struct.* **29**, 439–461
45. De Castro, L.F. and Zacharias, M. (2002) DAPI binding to the DNA minor groove: a continuum solvent analysis. *J. Mol. Recognit.* **15**, 209–220
46. Reinert, K.E. (1999) DNA multimode interaction with berenil and pentamidine; double helix stiffening, unbending and bending. *J. Biomol. Struct. Dyn.* **17**, 311–331
47. Pilch, D.S., Kirolos, M.A., Liu, X., Plum, G.E., and Breslauer, K.J. (1995) Berenil [1, 3-bis(4(-amidinophenyl)triazene] binding to DNA duplexes and to a RNA duplex: evidence for both intercalative and minor groove binding properties. *Biochemistry* **34**, 9962–9976
48. Utsuno, K., Tsuboi, M., Katsumata, S., and Iwamoto, T. (2002) Visualization of complexes of Hoechst 33258 and DNA duplexes in solution by atomic force microscopy. *Chem. Pharm. Bull. (Tokyo)* **50**, 216–219
49. Matulis, D., Rouzina, I., and Bloomfield, V.A. (2002) Thermodynamics of cationic lipid binding to DNA and DNA condensation: roles of electrostatics and hydrophobicity. *J. Amer. Chem. Soc.* **124**, 7331–7342
50. Reimer, D.L., Zhang, Y., Kong, S., Wheeler, J.J., Graham, R.W., and Bally, M.B. (1995) Formation of novel hydrophobic complexes between cationic lipids and plasmid DNA. *Biochemistry* **34**, 12877–12883
51. Stokke, T. and Steen, H.B. (1986) Binding of Hoechst 33258 to chromatin in situ. *Cytometry* **7**, 227–234
52. Adhikary, A., Buschmann, V., Muller, C., and Sauer, M. (2003) Ensemble and single-molecule fluorescence spectroscopic study of the binding modes of the bis-benzimidazole derivative Hoechst 33258 with DNA. *Nucleic Acids Res.* **31**, 2178–2186